Bull. Inst. Chem. Res., Kyoto Univ., Vol. 67, No. 4, 1989

# A Tubular-Epithelium Model Constructed from a Gelatin Tube and Renal Epithelial Cells (MDCK)

Koji ASAMI*, Akihiko IRIMAJIRI** and Tetsuya HANAI*

*Received August 25, 1989*

An *in vitro* macro-model for tubular epithelial tissues was constructed. The Madin-Darby canine kidney (MDCK) cells were cultured on gelatin tubues of 1–2 mm diameter. The model was characterized by both histological and dielectric techniques, which revealed that cell monolayers covered totally the luminal and/or abluminal surfaces of the gelatin tubes. The specific capacitance and conductance of the tubular monolayers were estimated to be 1.6 $\mu Fcm^{-2}$ and 1–10 $mScm^{-2}$, respectively.

KEY WORDS: Dielectric dispersion/ Interfacial polarization/ Epithelial monolayer/ Cultured cell/ Monolayer capacity/ MDCK

## INTRODUCTION

The use of cell culture techniques enables us to study complex physiological processes in a relatively simple model system. In particular, the epithelial cell monolayers formed on planar permeable supports provide a useful model system to examine epithelial transport functions. The MDCK cell line derived from the dog kidney has been extensively studied in this respect. The MDCK monolayers in a planar form retained structural and functional properties similar to those of the renal tubules [1–3].

In this study, we constructed a tubular monolayer system, which has a more realistic configuration (as a model for the renal tubules) than the planar monolayer system. The integrity of the tubular monolayers was confirmed by histological and dielectric techniques.

## MATERIALS AND METHODS

*Cell culture*

The Madin-Darby canine kidney (MDCK) cells were grown in Dulbecco's modified Eagle's medium (DMEM) supplemented with 5% foetal calf serum and 100 mg/l kanamycin. The cells used in this experiment were in 63–70th passage.

*Preparation of gelatin tubes*

Stable gelatin tubes 1.8–2.0 mm in diameter were made of cross-linked gelatin hydrate. A 1.6 mm glass rod was dipped into a viscous solution of 10% gelatin to form a gel layer of 0.2–0.5 mm thick around the glass rod. The gelatin-coated rod was treated with a 2.5% glutaraldehyde solution for 30–60 min, which treatment provided

* 浅見耕司，花井哲也：Laboratory of Dielectrics, Institute for Chemical Research, Kyoto University, Uji, Kyoto 611.
** 入交昭彦：Department of Physiology, Kochi Medical School, Nankoku, Kochi 781–51.

mechanical stability for the gelatin layer. After the rod was transferred into water, the gelatin layer was slipped off from the rod. The resulting rubber-like tubes were rinsed thoroughly with distilled water and connected with silicon tubes as shown in Fig. 1.

*Monolayer formation*

The gelatin tubes were sterilized in 70% ethanol for 1 hr and placed in a dish containing the culture medium (DMEM). The cells, harvested with 0.05% trypsin-0.02% EDTA, were plated on the abluminal and/or luminal surface of the gelatin tubes. After 1–2 day culture, the cells formed monolayers over the gelatin support.

*Light microscopy*

Formation of the cell monolayers on the gelatin tubes was monitored under a phase-contrast microscope. Cross-sectional images of the monolayered tubes were obtained with cryostat sections stained with hematoxylin.

*Dielectric measurements*

A gelatin tube with or without a cell-monolayer mounted on a holder was sandwiched between two platinized Pt electrodes glued onto lucite plates (Fig. 2). This system

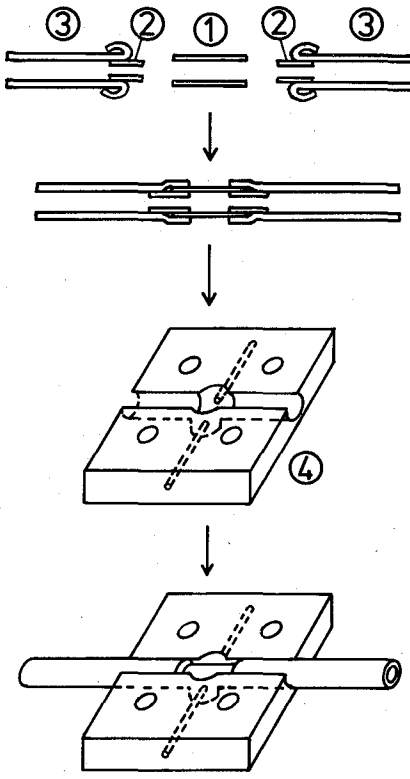


Fig. 1. A gelatin tube (1) is connected with silicon tubes (3) via glass capillary joints (2) and is mounted on a lucite holder (4).

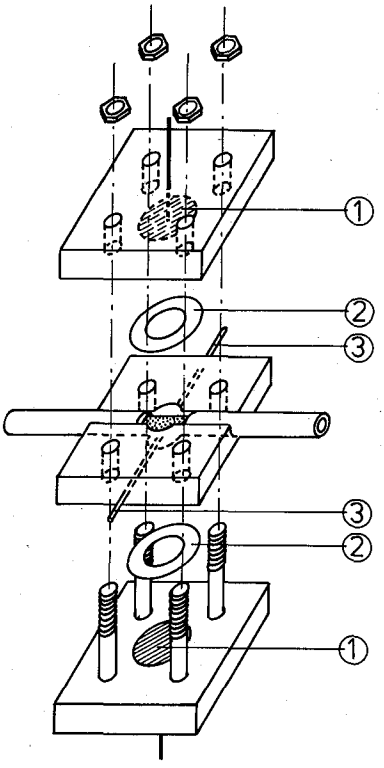


Fig. 2. Exploded view of the chamber used for dielectric studies of tubular monolayer systems. A tube mounted on a holder is positioned between platinized Pt electrodes. (1) Pt electrodes, (2) sealing films, and (3) stainless steel tubes for circulation of the medium in the chamber.

was connected to an HP 4192A Impedance Analyzer, and the equivalent parallel capacitance and conductance were measured over a frequency range 10 Hz to 10 MHz, as described previously [4, 5]. During the measurements, the luminal and abluminal solutions were perfused and their conductivities were simultaneously monitored with

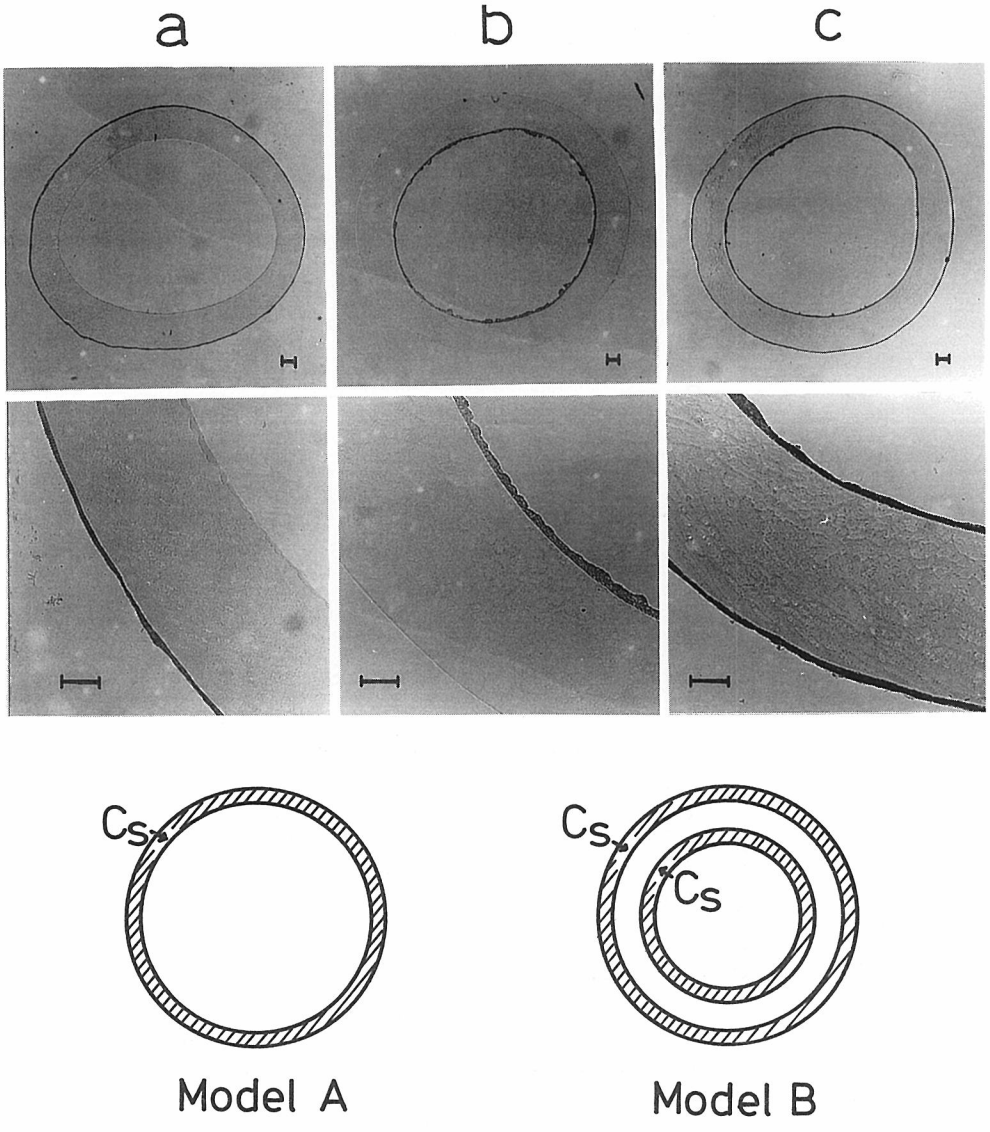


Fig. 3. Cross-sectional views of three types of tubular monolayer systems and schematic diagrams of the related dielectric models. The three systems are (a) abluminal monolayer, (b) luminal monolayer, and (c) abluminal/luminal double monolayers. Scale bars indicate 0.1 mm. In the two dielectric models, a relatively conducting cylinder has a poorly conducting layer (in model A) or two poorly conducting layers (in model B). $C_s$ is the specific capacitance of the layers (or the monolayers).

two flow-through type cells connected to an HP 4275A Multi Frequency LCR Meter. The luminal and abluminal solutions used were DMEM and 10% DMEM, respectively. Both solutions contained 10 mM Hepes-NaOH (pH 7.4) and their osmolarities were adjusted to 280 mosM with mannitol.

## RESULTS AND DISCUSSION

By plating the MDCK cells on either one side or both sides of the gelatin tubes, we prepared the following three types of tubular monolayer systems: (a) abluminal monolayer, (b) luminal monolayer and (c) abluminal/luminal double monolayers. Figure 3 shows the cross-sectional view of these systems after 1–2 day culture. The cell monolayers stained with hematoxylin were represented by a single or double continuous lines 5–10 $\mu$m thick along a less stained gelatin substrate. The intercellular borders in the monolayers were not clearly seen in the photomicrographs. Thus, the histological results indicate that the cells encompassed the gelatin tubes leaving no free space and

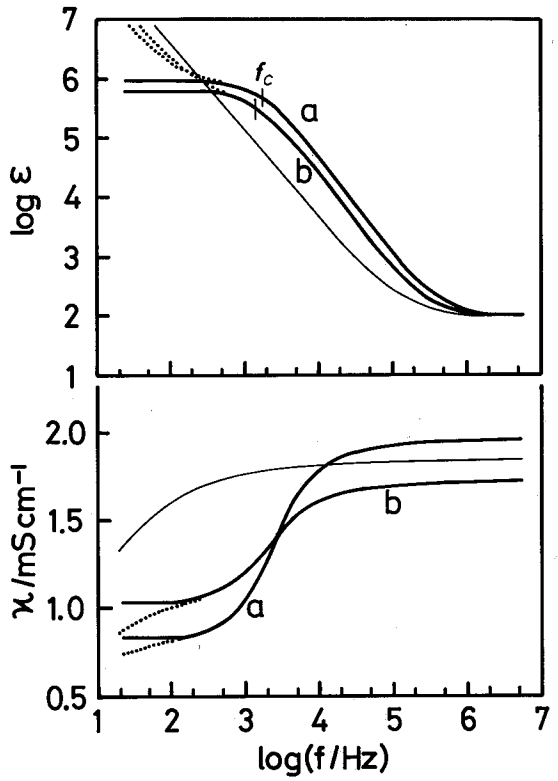


Fig. 4. Frequency dependence of the relative permittivity and conductivity of two single-monolayer systems: abluminal monolayer (Curve a) and luminal monolayer (Curve b). The solid lines indicate the subtractions of the artifactual components due to electrode polarization effect from raw data (dotted lines). The vertical bars on the permittivity curves indicate characteristic frequencies. The thin lines refer to the data of a gelatin tube without a monolayer as a control.

that the adjacent cells tightly joined each other.

In order to characterize the passive electrical properties of the monolayers, these three systems were subjected to dielectric measurements. Figure 4 shows the results obtained with the two types of single-monolayer systems. Dielectric dispersions with a single characteristic frequency were observed for both the abluminal and luminal monolayer systems. According to the dielectric theory based on model A in Fig. 3 that a conducting cylinder is covered with a poorly conducting layer, we determined the monolayer capacitance ($C_s$) from the dielectric data. The calculation method is described in Appendix. The monolayer capacitance (1.6 $\mu$Fcm$^{-2}$) obtained for the two systems was in good agreement with that of planar monolayers cultured on permeable substrates (1.8 $\mu$Fcm$^{-2}$ from a.c measurements by Asami et al. [6] and 1.4 $\mu$Fcm$^{-2}$ from d.c. transient measurements by Cereijido et al. [7]).

In contrast with the single-monolayer systems, the abluminal/luminal double-monolayer system showed a wide-spread dispersion, in which the permittivity and conductivity curves were reproduced by a superposition of two subdispersions with characteristic frequencies $f_{c1}$ and $f_{c2}$ (Fig. 5). This dielectric dispersion was explained by the dielectric theory based on model B in Fig. 3 that a conducting cylinder is covered with two poorly conducting layers separated by a conducting layer. Thus, the dielectric dispersion technique, even without recourse to a histological examination, could detect structure differences between the single- and double-monolayer systems.

Since the monolayer conductance cannot be determined from the dielectric dispersions observed from outside the tubes, we measured it directly across the monolayers by using a Pt wire electrode inserted into the lumen. When a serum-free DMEM was employed as the abluminal and luminal solutions, the conductance of the monolayers

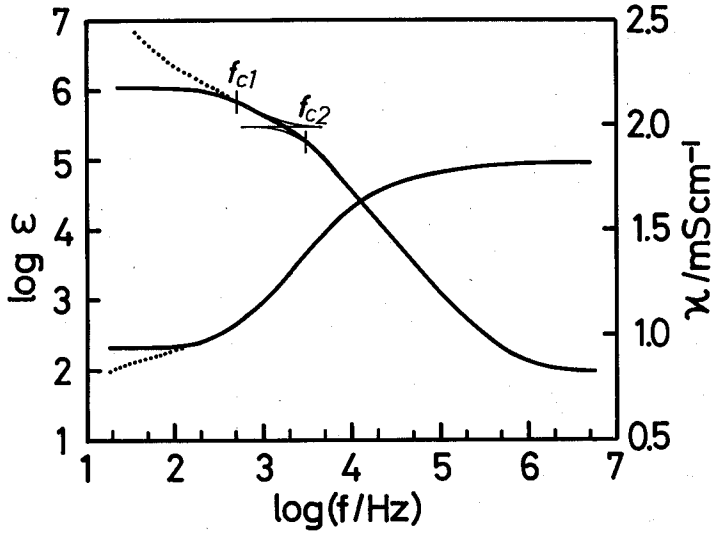


Fig. 5. Dielectric dispersion curves obtained for a double-monolayer system. The solid lines are simulated by a superposition of two Cole-Cole type dispersions with characteristic frequencies $f_{c1}$ and $f_{c2}$. Dotted lines are uncorrected data for electrode polarization.

was within a range of 1 to 10 $mScm^{-2}$, being in agreement with that of planar monolayers (1–10 $mScm^{-2}$ obtained by Asami et al. [6], 10 $mScm^{-2}$ by Misfeldt et al. [1] and Cereijido et al. [2] and 0.24 $mScm^{-2}$ by Simons [3]).

## CONCLUSION

We constructed tubular epithelial monolayers supported by cross-linked gelatin hydrate. Histological and dielectric techniques confirmed the integrity of the tubular monolayers; i.e., the cells formed continuous monolayers on the abluminal and/or luminal surface of the gelatin tubes and their passive electrical properties were consistent with those of the planar monolayers. Hence, this technique enables us to use the tubular monolayers as an *in vitro* macro model for tubular epithelial tissues.

## ACKNOWLEDGMENTS

We would like to thank Dr. Y. Kinoshita for his helpful discussion. We also acknowledge Mrs. T. Ichinowatari and Mr. K. Yagiu for their expert technical assistance.

## APPENDIX

We drive equations concerning the complex permittivity ($\varepsilon_t^*$) of the system that a cylinder (of the complex permittivity $\varepsilon_i^*$) with a single layer ($\varepsilon_s^*$) is placed in a continuous medium ($\varepsilon_a^*$) (see Fig. 6). Here, the complex permittivities are defined as $\varepsilon^*=\varepsilon-j\kappa/\omega\in_v$, where $\varepsilon$ is relative permittivity, $\kappa$ is conductivity, $\omega=2\pi f$, $f$ is frequency, $\in_v$ is permittivity of vacuum, and $j=\sqrt{-1}$. When an electric field is applied perpendicular to the longitudinal axis of the cylinder, $\varepsilon_t^*$ is given by

$$\varepsilon_t^*=\varepsilon_a^*\frac{\varepsilon_a^*+\varepsilon_p^*-\Phi(\varepsilon_a^*-\varepsilon_p^*)}{\varepsilon_a^*+\varepsilon_p^*+\Phi(\varepsilon_a^*-\varepsilon_p^*)}, \tag{1}$$

$$\varepsilon_p^*=\varepsilon_s^*\frac{\varepsilon_s^*+\varepsilon_i^*-v(\varepsilon_s^*-\varepsilon_i^*)}{\varepsilon_s^*+\varepsilon_i^*+v(\varepsilon_s^*-\varepsilon_i^*)}, \tag{2}$$

where $\Phi$ is volume fraction, $v=[R/(R+d)]^2$, $R$ is the radius of the cylinder, and $d$ is the thickness of the layer. Equations 1 and 2 can be rewritten as:

$$\varepsilon_t^*=\varepsilon_h+\frac{\Delta\varepsilon_p}{1+j\omega\tau_p}+\frac{\Delta\varepsilon_q}{1+j\omega\tau_q}+\frac{\kappa_l}{j\omega\in_v}. \tag{3}$$

The dielectric parameters—$\varepsilon_h$, $\Delta\varepsilon_p$, $\Delta\varepsilon_q$, $\tau_p$, $\tau_q$, and $\kappa_l$—are given by

$$\varepsilon_h=\varepsilon_a\frac{B}{D}, \tag{4}$$

$$\Delta\varepsilon_p=\frac{\in_v\varepsilon_a-\kappa_a\tau_p}{\in_v C(\tau_p-\tau_q)\tau_p}(A\tau_p^2-E\tau_p+B), \tag{5}$$

$$\Delta\varepsilon_q=\frac{\in_v\varepsilon_a-\kappa_a\tau_q}{\in_v C(\tau_p-\tau_q)\tau_q}(-A\tau_q^2+E\tau_q-B), \tag{6}$$

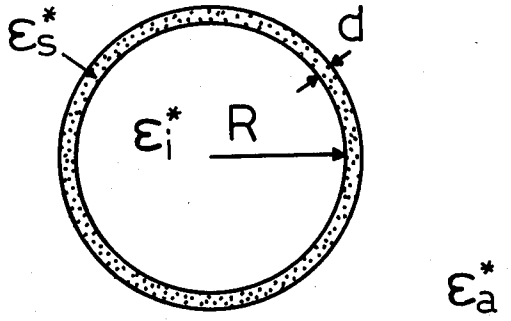


Fig. 6. A dielectric model for a cylinder covered with a single layer (A cross-sectional view is shown). $\varepsilon^*$ is complex permittivity defined as: $\varepsilon^*=\varepsilon-j\kappa/\omega\in_v$, where $\varepsilon$ is relative pemittivity, $\kappa$ is conductivity, $\omega=2\pi f$, $f$ is frequency, and $\in_v$ is permittivity of vacuum. $R$ is the radius of the cylinder and $d$ is the thickness of the layer. Subscripts $a$, $s$, and $i$ are refer to the external, layer and inner phases, respectively.

$$\tau_p=\frac{F+\sqrt{F^2-4CD}}{2C}, \tag{7}$$

$$\tau_q=\frac{2D}{F+\sqrt{F^2-4CD}}, \tag{8}$$

$$\kappa_l=\kappa_a\frac{A}{C}, \tag{9}$$

where

$$a=(1+v)\,\kappa_i+(1-v)\,\kappa_s, \tag{10}$$
$$b=(1-v)\,\kappa_i+(1+v)\,\kappa_s, \tag{11}$$
$$c=(1+v)\,\varepsilon_i+(1-v)\,\varepsilon_s, \tag{12}$$
$$d=(1-v)\,\varepsilon_i+(1+v)\,\varepsilon_s, \tag{13}$$
$$A=a\,(1+\Phi)\,\kappa_s+b\,(1-\Phi)\,\kappa_a, \tag{14}$$
$$B=[c\,(1+\Phi)\,\varepsilon_s+d\,(1-\Phi)\,\varepsilon_a]\,\in_v^2, \tag{15}$$
$$C=a\,(1-\Phi)\,\kappa_s+b\,(1+\Phi)\,\kappa_a, \tag{16}$$
$$D=[c\,(1-\Phi)\,\varepsilon_s+d\,(1+\Phi)\,\varepsilon_a]\,\in_v^2, \tag{17}$$
$$E=[(1+\Phi)(a\varepsilon_s+c\kappa_s)+(1-\Phi)(b\varepsilon_a+d\kappa_a)]\,\in_v, \tag{18}$$
$$F=[(1-\Phi)(a\varepsilon_s+c\kappa_s)+(1+\Phi)(b\varepsilon_a+d\kappa_a)]\,\in_v. \tag{19}$$

Equation 3 indicates that $\varepsilon_t^*$ has two dielectric relaxation regions: $P$- and $Q$-relaxation. The tubular monolayer systems of interest hold the following assumptions: $\kappa_s\ll\kappa_a$, $\kappa_s\ll\kappa_i$ and $d\ll R$. In such cases, $\varepsilon_t^*$ is simply represented by

$$\varepsilon_t^*\simeq\varepsilon_h+\frac{\Delta\varepsilon_p}{1+j\omega\tau_p}+\frac{\kappa_l}{j\omega\in_v}. \tag{20}$$

The dielectric parameters—$\varepsilon_h$, $\Delta\varepsilon_p$, $\tau_p$, and $\kappa_l$—are approximately given by

$$\varepsilon_h \simeq \varepsilon_a, \tag{21}$$

$$\Delta\varepsilon_p \simeq \frac{4C_s R\Phi}{(1+\Phi)^2 \in_v}, \tag{22}$$

$$\tau_p \simeq C_s R\left(\frac{1-\Phi}{1+\Phi}\frac{1}{\kappa_a}+\frac{1}{\kappa_i}\right), \tag{23}$$

$$\kappa_l \simeq \kappa_a \frac{1-\Phi}{1+\Phi}, \tag{24}$$

where the specific capacitance of the layer, $C_s$, is defined as $C_s=\frac{\varepsilon_s \in_v}{d}$. Equations 22 and 24 are rewritten as follows:

$$C_s \simeq \frac{(1+\Phi)^2 \in_v}{4R\Phi}\Delta\varepsilon_p, \tag{25}$$

$$\Phi \simeq \frac{1-\kappa_l/\kappa_a}{1+\kappa_l/\kappa_a}. \tag{26}$$

Thus, the capacitance of the layer $C_s$ and volume fraction $\Phi$ are calculated from the parameters $\Delta\varepsilon_p$, $\kappa_l$, $\kappa_a$ and $R$, which are all experimentally observable.

## REFERENCES


1) D. S. Misfeldt, S. T. Hamamoto and D. R. Piteka, *Proc. Nat. Acad. Sci. USA*, **73**, 1212–1216 (1976).
2) M. Cereijido, E. S. Robbins, W. J. Dolan, C. A. Rotunno, and D. D. Sabatini, *J. Cell Biol.*, **77**, 853–880 (1978).
3) N. L. Simmons, *J. Membrane Biol.*, **59**, 105–114 (1981).
4) K. Asami and A. Irimajiri, *Biochim. Biophys. Acta*, **769**, 370–376 (1984).
5) K. Asami and A. Irimajiri, *Bull. Inst. Chem. Res. Kyoto Univ.*, **63**, 259–275 (1985).
6) K. Asami, A. Irimajiri and T. Hanai, The 1987 International Congress on Membrane and Membrane Processes, Tokyo, Japan (abstract). pp. 196–197 (1987).
7) M. Cereijido, E. Stefani and A.M. Palomo, *J. Membrane Biol.* **53**, 19–32 (1980).